Chapter

Effects of Dispersed Sulfides in Bronze During Sintering

Tomohiro Sato

Abstract

Bronze material sintered as sliding bearing is used. In particular, lead bronze is often used because lead acting as a solid lubricant has excellent friction characteristics. However, lead was replaced by another material according to environmental regulations. One candidate for a lead-free material is a sulfide that is well known as a solid lubricant. In this chapter we describe sintering properties and their mechanical properties. First, we investigate chemical components of copper sulfide system and realize stable phase in bronze matrix. After that, we consider the sintering condition of bronze with sulfide dispersed. The sulfides in the bronze may be subject to chemical reduction during sintering, especially when this is carried out under a reducing atmosphere containing hydrogen gas. The effect of the sulfides on the bronze, with a focus on the hardness of the bronze matrix and the reaction between sulfides and hydrogen gas, was investigated. Not only sinterability but also mechanical properties as hardness are discussed.

Keywords: sintering, Cu alloy, bronze, sulfide, hardness, friction

1. Introduction

Copper alloys based on copper and tin are useful materials as the so-called bronze (Cu-Sn alloy). For example, sliding bearings are common in industrial applications. These bearings are often manufactured using a sintering process in the field of powder metallurgy. Specifically, 90 Cu-10 Sn mass% bronze is common and has been developed and manufactured as a base materials of a bearing component.

Lead is a common element for use as industrial additives. This is also an indispensable material for additives for metal casting of Cu alloys and solders. The addition of lead ensures that the pressure resistance of the bronze and brass water devices and the mechanical properties of the solder are maintained. Lead is also useful in the manufacturing process. For example, lead made castability improve in the metal casting method [1, 2], and solderability is also improved due to low melting point of lead [3]. Lead has important applications as a solid lubricant, and lead bronze is a useful material for sliding bearings even though there are many regulations as RoHS and REACH and so on.

However, lead is harmful for human health, especially children and pregnant women. For that reason, various regulations are implemented to protect people.

These regulations or trends will affect industrial manufacturers. As a result, many industries have developed new materials as substitutes for lead.

Bismuth and sulfides are well known as lead substitutes and are candidates for the development of solid lubricants. Bi-bronze castings were used as bimetallic bearings and showed good loading capacity [4]. Potential applications of these castings are pointed out in Ref. [4], and it has been shown that castability was improved using Bi. The machinability of bronze-containing sulfides (Cu_2S and ZnS) was investigated. It was concluded that the mechanical properties and machinability of sand casting are the same as the mechanical properties and machinability of Pb-bronze castings [5]. For industrial, it is important that the manufacturing cost is low and that there is a stable supply of raw materials. Bi is far more expensive than S and Cu. Since Bi is a rare metal, the supply of sulfide seems to be superior to that of Bi. As a result, sulfide based on S and Cu is a promising alternative for lead substitution material.

In this study, we will discuss how to influence bronze sulfide which is already atomized. Specifically, the strength of bronze matrix and the reaction between sulfide and hydrogen gas are drawing attention. We clarify composition and atmosphere effective for sintering bronze with sulfide dispersed. In the investigation, solid-state sintering and liquid-phase sintering are compared under reducing atmosphere and inert atmosphere. Hardness as one of the important mechanical properties was also investigated. Moreover, some other sintering conditions and friction properties are also discussed.

2. Chemical component of sulfide-dispersed bronze

As shown in **Figure 1**, a phase diagram was calculated based on the calculation of phase diagrams (CALPHAD) method [6] of the Cu-Sn-Fe-S system in order to confirm the optimum content of the sulfide in the cast material. In the Cu-Sn alloy, since the crystallization of the α′ phase of Fe was suppressed, the Fe content was 1.3 mass% or less. The reason why the sulfide was dispersed in the Cu alloy is that crystallization of the sulfide (0.25 mass% or less) occurred after crystallization of the α-phase Cu. On the one hand, the sulfide in the matrix remained below 0.60% by mass experimentally. **Figure 2** shows the matrix and sulfides of casting alloys [7].

On the other hand, much amount of sulfide is able to disperse in the atomized bronze powders. Because of the rapid cooling of (gas and/or water) atomization, atomized bronze keeps their metastable state including sulfide.

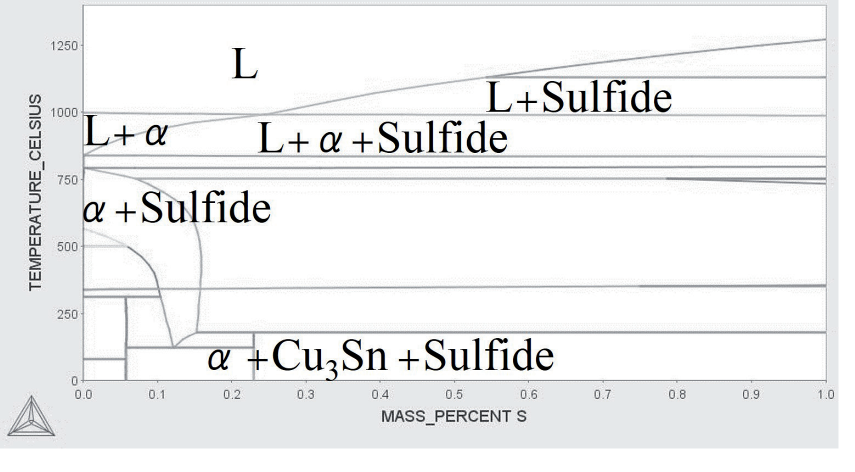

Figure 1.
Calculated phase diagram of sulfide bronze [7].

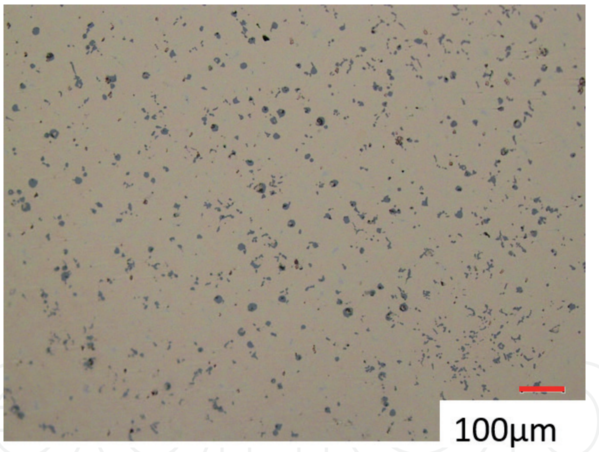

Figure 2.
Microstructure of sulfide bronze of castings.

3. Sintering process of sulfide bronze as bimetal

In this chapter, one of the conditions is the proposal of the copper alloy developed as the sliding member described below.

In the case of a Cu alloy containing a sulfide, sulfur may disappear from the Cu alloy by reacting with the reducing gas. Further, in the case of Cu-Sn-S, the mechanical properties of the sintered body have not been clarified. Therefore, hardness is evaluated as one of the mechanical properties.

3.1 Materials

Atomized powders were prepared for comparison of sintering properties. As a feature of the sulfide-dispersed Cu-Sn system materials, the sulfide was pre-alloyed by water atomization manufacturing. As shown in **Figure 3a–e**, micro-sized small dots were observed by scanning electron microscopy (SEM). This image is a sectional view of one of the typically sintered bronze-containing sulfides (from irregular powders). Generally, sintered composite from premixed bronze and sulfides indicated lower mechanical properties. It was reported that mechanical properties become better to cover the MoS_2 particles by copper [8]. However, this sulfide-dispersed bronze was made by atomizing as pre-alloyed material. So we can see that the pre-alloyed material shows better mechanical properties than the premixed material.

Energy-dispersive X-ray spectroscopy (EDS) was performed to determine the elements that make up the observed small dots. As a result, as shown in **Figure 1**, a ternary sulfide consisting of Cu, Fe, and S was detected. This sulfide is a kind of bornite (Cu_5FeS_4) detected by the X-ray diffraction (XRD) method [9] as shown in **Figure 4**. Only a small peak was observed as bornite (dot references). It may be metastable in the system because it is difficult to crystalize in the phase diagram as shown in **Figure 1**.

3.2 Experimental method

3.2.1 Sintering and manufacturing process

By preparing, bimetal specimens, these procedures are conducted as below.

At first, powder was sprayed to a height of 1.0 mm (by leveling off) onto a 3.2-mm-thick steel plate (low-carbon steel). At this time, binding materials such

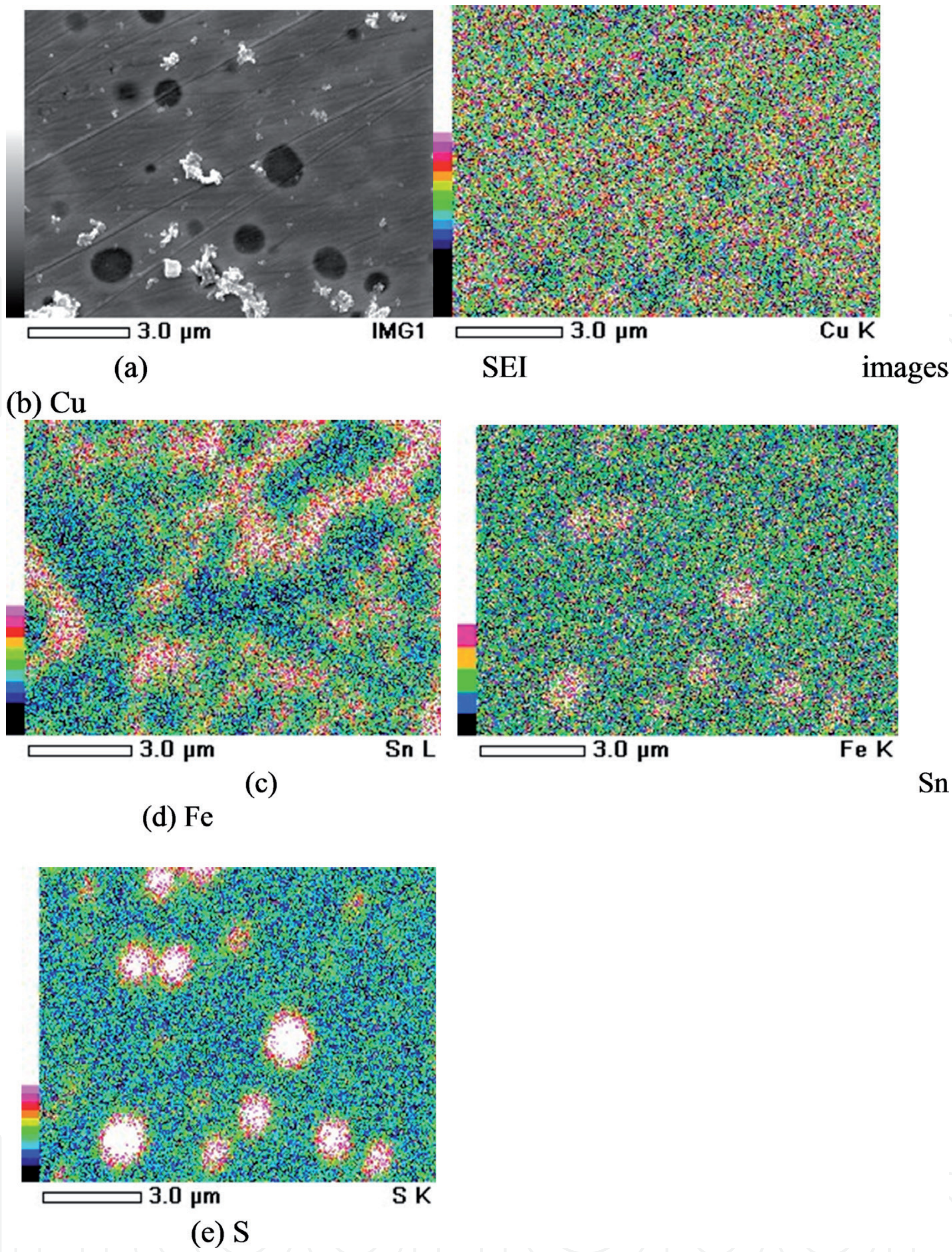

Figure 3.
SEM image of and EDS mapping results for the sulfide-dispersed copper alloy [10].

as oils or zinc stearate were not mixed. As the next step, the first sintering under reducing and/or inert atmosphere is performed.

The sample was heated to 1123 K for 1050 s in a mesh belt furnace. Next, the thickness of the bimetal was adjusted by a cold rolling mill. The thickness of the bimetal was controlled to flatten the entire surface on the Cu side of the bimetal in contact with the roll surface. Then, a second sintering under reducing and/or inert atmosphere is performed. The sample was heated to 1123 K for 1368 s in a mesh belt furnace.

After these procedures, to the analysis of mechanical properties, hardness tests were conducted because the bimetals and sintered copper alloy specimens were too thin to be subjected to tensile tests. The hardness of the sintered copper alloy specimens was evaluated using a Vickers hardness meter. This testing machine uses

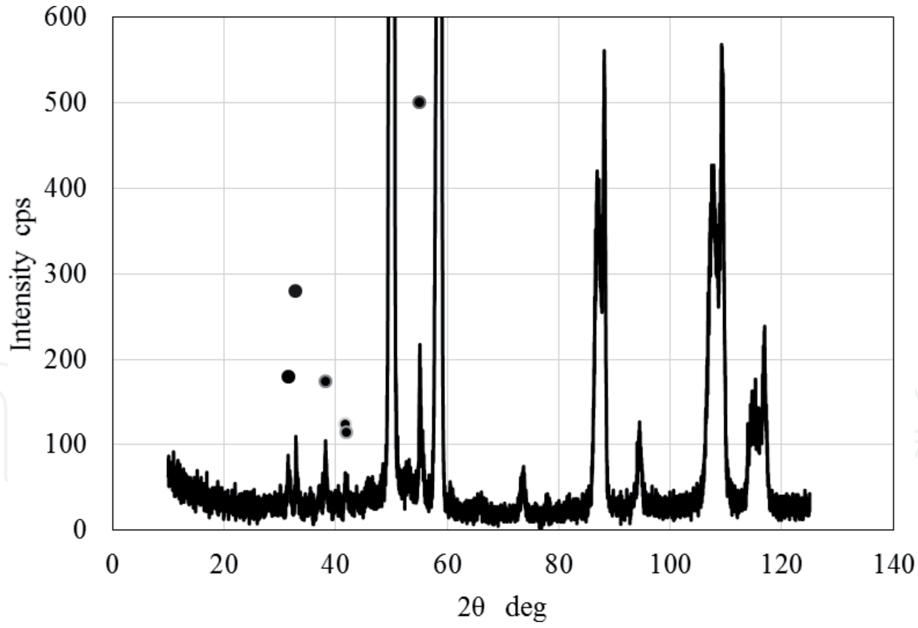

Figure 4.
XRD of sulfide-dispersed bronze powders.

a regular square pyramid diamond indenter with a face-to-face angle of 136° and a pyramid-shaped hollow on the test surface.

The hardness represented by a value obtained by dividing the load at that time by the surface area obtained from the length of the diagonal line of the permanent indentation is the Vickers hardness. The indenter was pushed into the matrix of the copper alloy and the steels under an applied load of 0.98 N for 10 s.

3.2.2 Test specimens

Six test specimens were prepared for observation of the sintering process, as shown in **Table 1**. In the table, the chemical components are described only for the primary element (i.e., Cu, Sn, Fe, S, and sulfide). Here, with respect to the sulfide concentration, all sulfur was assumed to exist as bornite.

As preliminary alloy powders for solid-phase sintering at the time of initial-stage sintering, SB8 (sulfide bronze containing 8 mass% Sn), SB10, and SB12 were used. However, SBP8 (sulfide bronze using a premix containing 8% by mass Sn), SBP10, and SBP12 are the same pre-alloyed powders as used in the first sintering (SB8, SB10, SB) (prepared as a mixture of 12). Bronze (containing 20% by mass Sn) powder. These mixed powders are prepared for liquid sintering at the time of primary sintering. The addition of low-melting Cu-Sn powder during the sintering process was tried experimentally to improve sintering [10].

Materials		Cu	Sn	Fe	S	Sulfide
SB	8	Bal.	7.90	0.18	0.31	1.21
	10	Bal.	9.52	0.38	0.48	1.88
	12	Bal.	12.00	0.41	0.58	2.27
SBP	8	Bal.	8.00	0.13	0.20	0.78
	10	Bal.	10.00	0.15	0.26	1.02
	12	Bal.	12.00	0.29	0.37	1.45

Table 1.
Chemical composition of powders primary elements (mass%) [10].

3.2.3 Test conditions

The sintering temperature was kept at 1123 K, as described in Section 3.2.1. This temperature made Cu-Sn system in liquid state so that liquid sintering was conducted for SBP8, SBP10, and SBP12. The mesh belt speed was set at 0.43 mm/s (first sintering) and 0.33 mm/s (second sintering). So, test specimens were maintained at 1123 K for 1050 s during the first sintering and for 1368 s during the second sintering. These sinterings were conducted under only reducing atmosphere (indicated as a after the materials in **Table 1**), only inert atmosphere (indicated as b after the materials in **Table 1**), and mixed atmosphere. Some tests were conducted using a complex procedure. They were sintered under inert gas during the first sintering and under reducing gas during the second sintering (indicated as c after the materials in **Table 1**). Under the reducing atmosphere, not only oxygen but also sulfur was able to reduce. Here, the reducing atmosphere was a mixture of H_2 gas and N_2 gas, and the inert atmosphere consisted only of N_2 gas. Sulfur in bronze may react as H_2S in the reducing gas. Thus, sintering under an inert atmosphere was also performed to compare the states of sulfur and sulfide bronze. Between the first and the second sinterings, a rolling process was performed, and the thickness of the bimetal was controlled to level the all surface of the Cu side of the bimetal contacted with the roll surface.

3.3 Results and discussion

3.3.1 First sintering

Figure 5 shows the results of optical microscopy observations. Specimens SB8a **Figure 5a**, SBP8a **Figure 5d**, SBP10a **Figure 5e**, and SBP12a **Figure 5f** were well sintered and contained few pores. Specimens SB10a **Figure 5b** and SB12a **Figure 5c** were difficult to observe because the sintered copper layer and steel were not adhered. Previous research has shown that the grain boundaries in copper alloys almost match the boundaries of individual particles (atomized powders); thus, diffusion may occur only at the surface of the particles because many sulfide dots remain in the Cu matrix. However, specimen SB8a had no grain boundaries. This is because of the

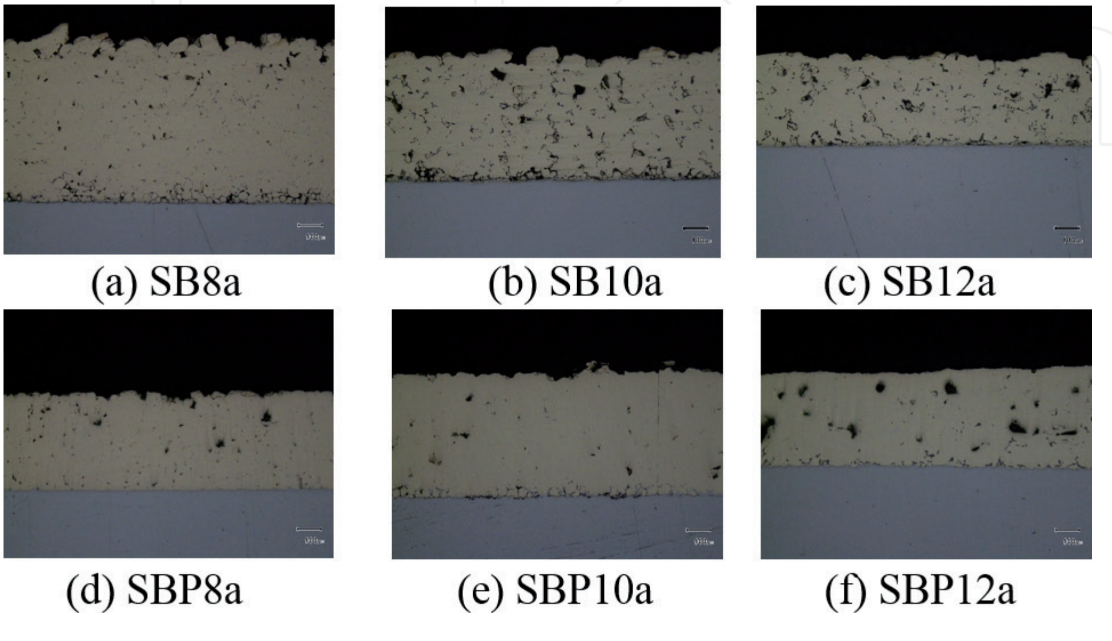

Figure 5.
Sectional view of sintered bimetal specimens after their first sintering under a reducing atmosphere [10].

differences between the sulfur content used in the previous study (S = 2 mass%) and that used in this study (S = 0.3 mass%).

In the cases of SBP8, SBP10, and SBP12, our results are similar to those reported in a previous study conducted under batch furnace conditions. Since the Cu-20 Sn powder begins to melt at 1071 K, effective diffusion is caused by liquid-phase sintering in Cu-Sn, since it is lower than the sintering temperature of 1113 K used in this study. **Figure 6a–e** shows the results of optical microscope observation of bimetal SB series and SBP series sintered in inert atmosphere. Samples SB8inr, SB10inr, SB10inr, SBP8inr, SBP10inr, and SBP12inr were well sintered and showed little pores.

In the sintered bronze, a dark brown network that appeared to comprise sulfide was present to a greater extent than in the specimens treated under a reducing atmosphere. At the reduction atmosphere, sulfur-containing sulfides in the copper alloy were apparently reduced and converted into H_2S gas in the furnace.

3.3.2 Second sintering under reduction atmosphere

Figure 7a–e shows the results of the bimetal after the second sintering under reducing atmosphere. Pores in the sintered copper alloy almost disappeared. However, as shown in **Figure 7b**, the alloy and the steel test piece did not adhere, and the sulfide almost disappeared from the test piece of the copper alloy.

In the second sintering process, the copper alloy samples were too sintered, which means that their pores almost disappeared. **Figure 8a–f** is a cross-sectional view of the test piece after the second sintering in an inert atmosphere. All copper alloy specimens were well sintered and almost void-free due to the rolling procedure performed between the first and second sinterings. The sulfide remained in the sample since the reaction in the sulfur in the sulfide is prevented because there is no reducing atmosphere.

3.3.3 Second sintering under complex atmosphere

Figure 9a–f is a cross-sectional view of a sintered bimetallic test piece after a second sintering in a reducing atmosphere and a sintered bimetallic test piece after

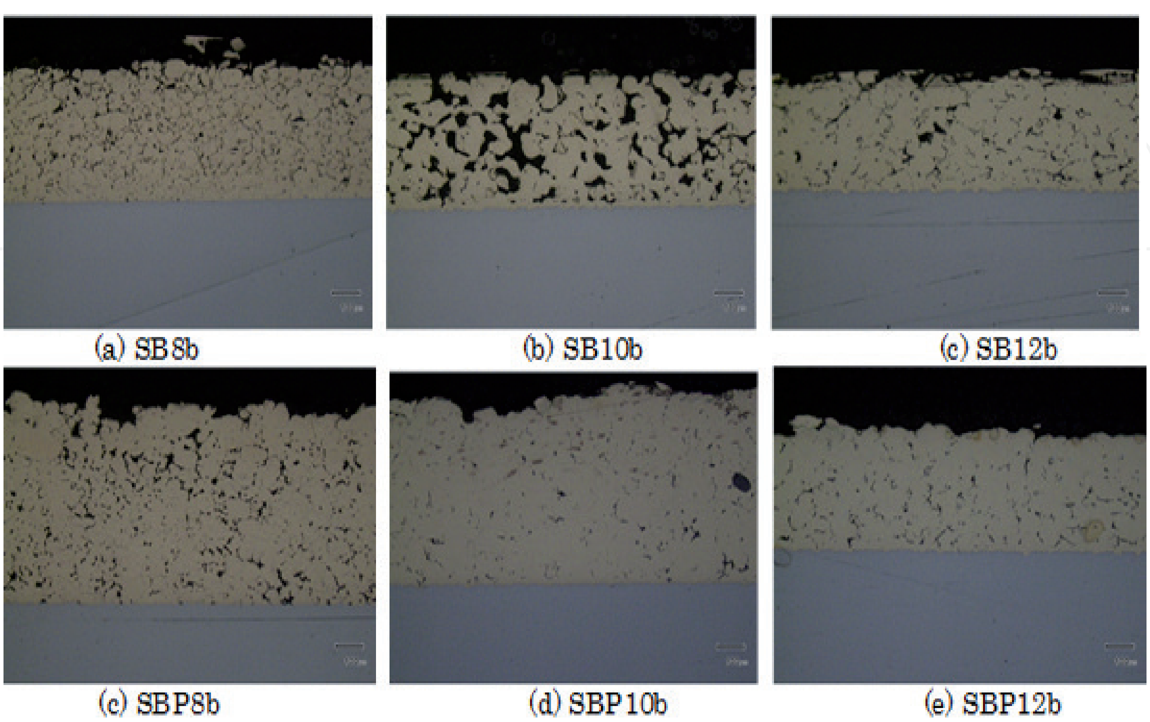

Figure 6.
Sectional view of sintered bimetal specimens after their first sintering under an inert atmosphere [10].

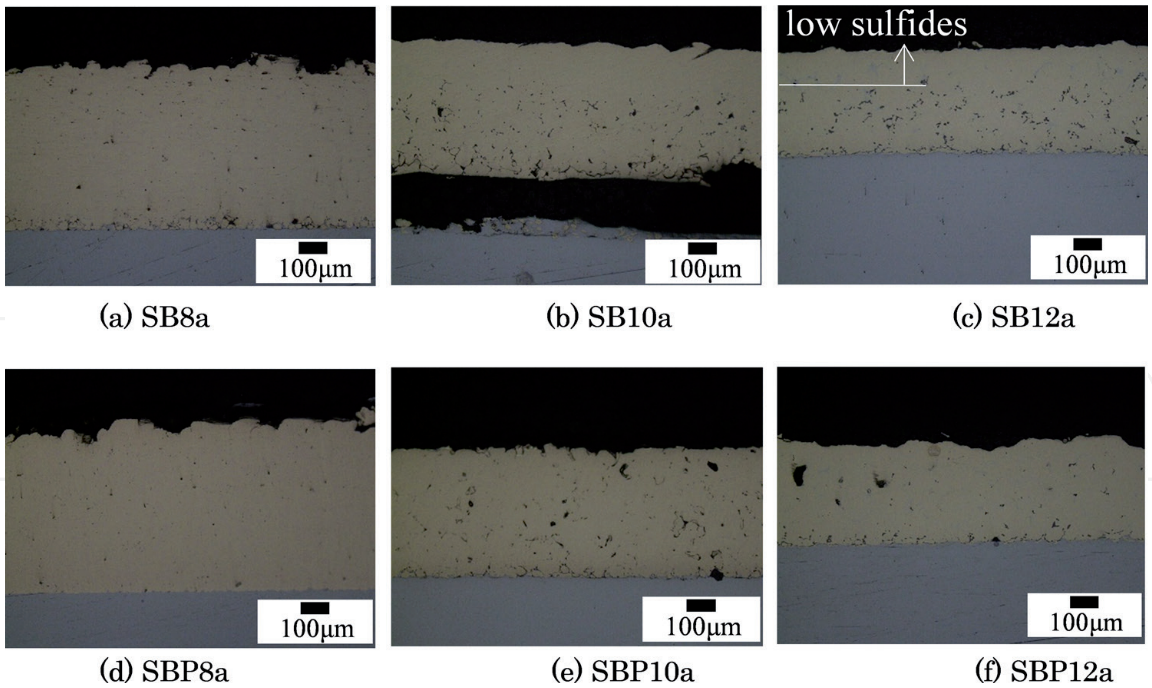

Figure 7.
Sectional view of sintered bimetal specimens after their second sintering under a reducing atmosphere [10].

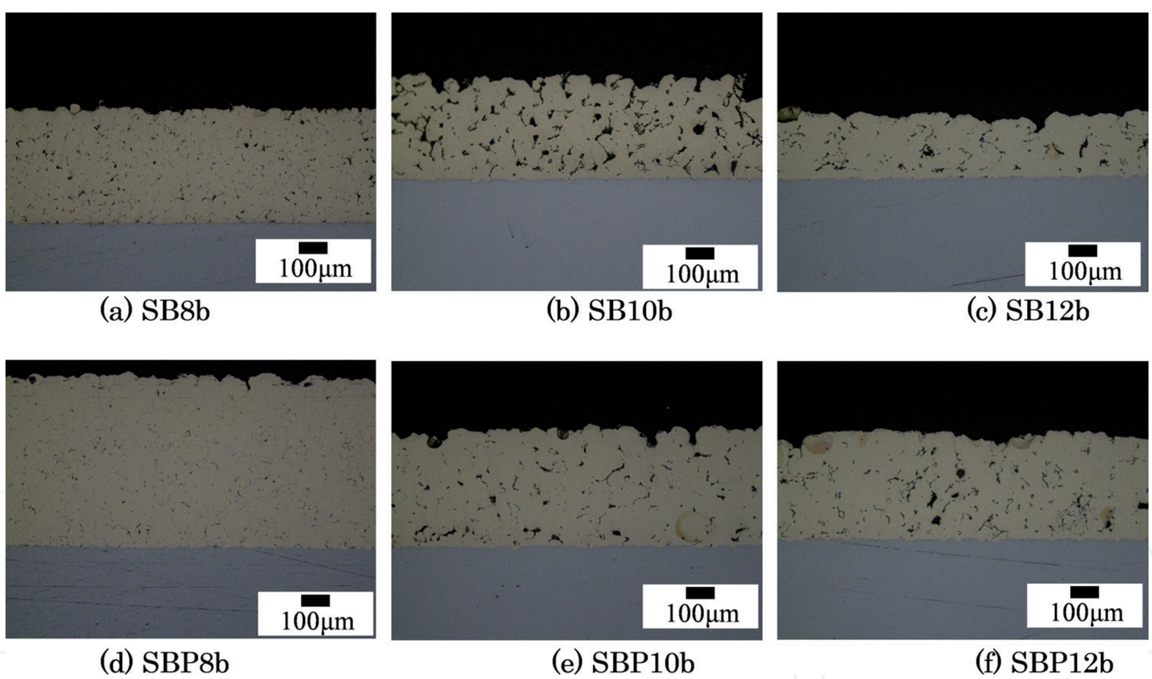

Figure 8.
Sectional view of sintered bimetal specimens after their second sintering under an inert atmosphere [10].

a first sintering in an inert atmosphere. The copper alloys in all the specimens were completely sintered and contained fewer pores than the specimens sintered only under inert atmosphere for both their primary and secondary sinterings. However, the sulfide content of the sintered bronze became inclined from the surface side to the interface side. So, a simple quantitative method of EDS was used for SPB10c.

As shown in **Figure 10a** and **b**, the sulfur on the front side disappeared, and in the simple quantitative method, only 0.2 mass% sulfur was detected. On the other hand, as shown in **Figure 10c** and **d**, the sulfur on the interface side remained, and 2.2% by mass of sulfur was detected. Therefore, the second sintering under reducing atmosphere resulted in the removal of sulfur from the surface of the copper alloy. Because the sulfide peak is small as shown in **Figure 4**, it

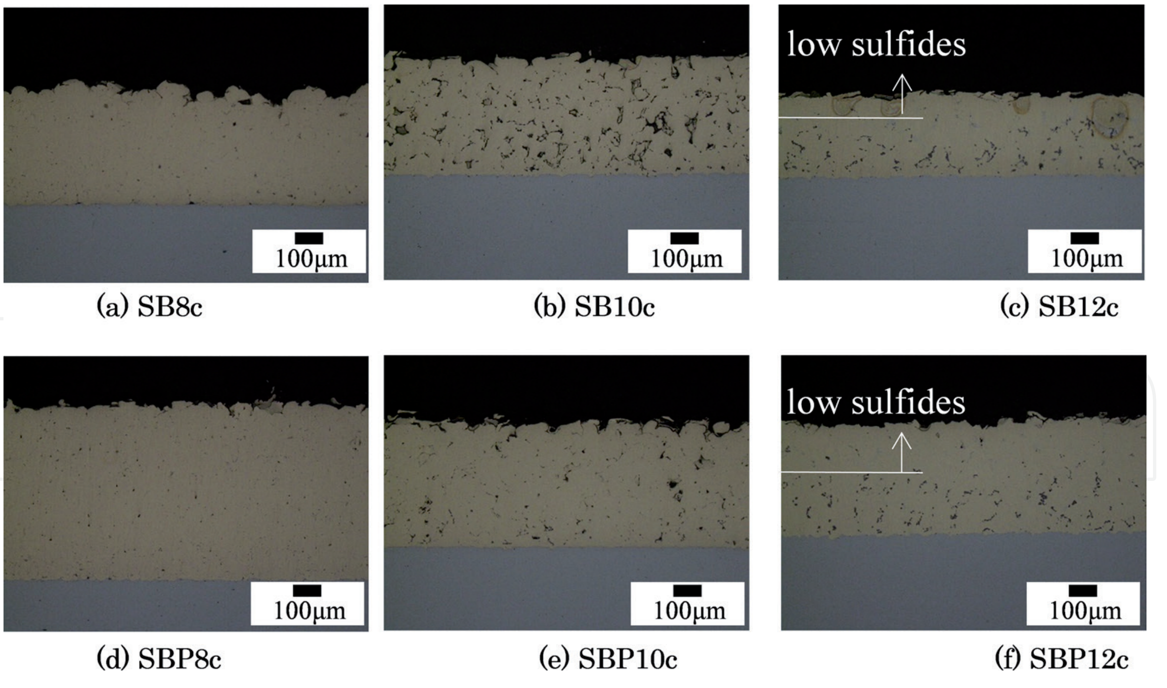

Figure 9.
Sectional view of sintered bimetal specimens after their second sintering under a reducing atmosphere [10].

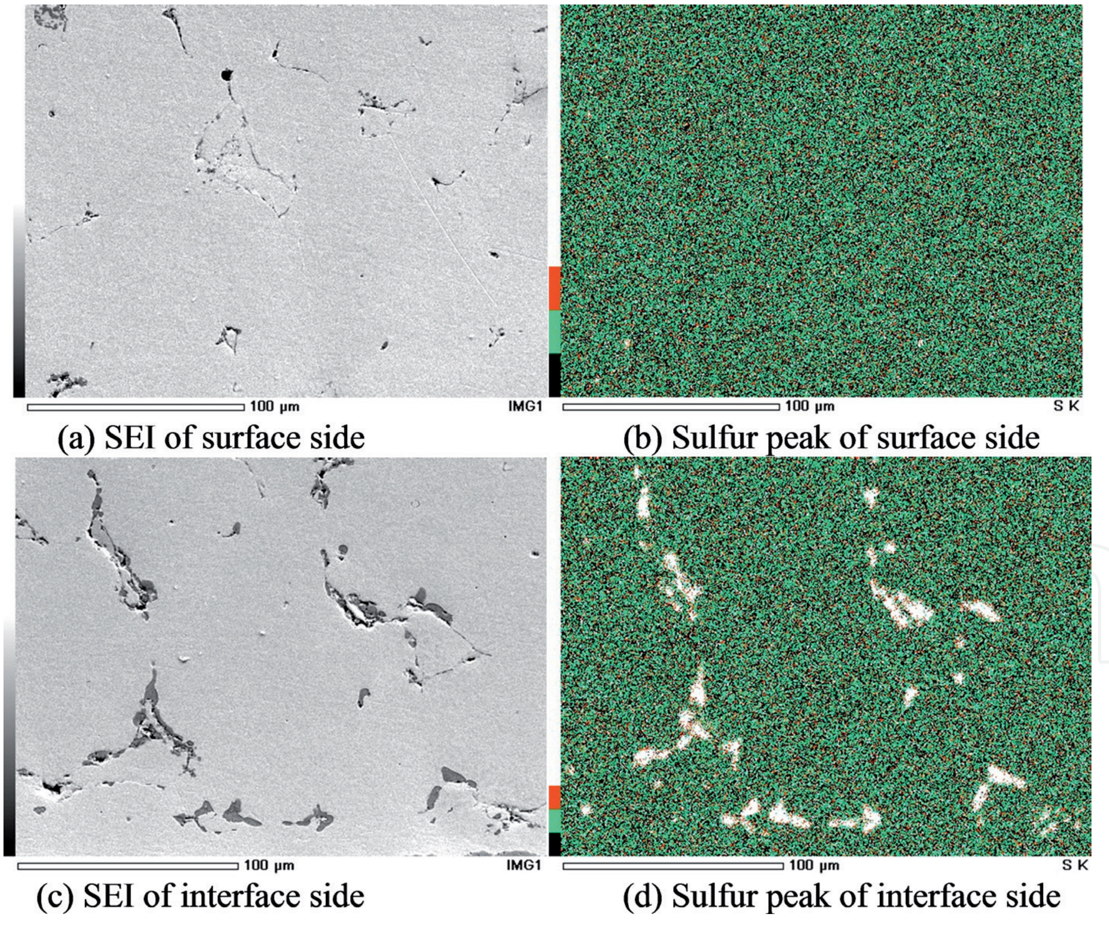

Figure 10.
SEI images and sulfur peak of SPB10c after their second sintering [10].

was difficult to detect sulfide by XRD in the cross section of bimetal. Therefore, apply EDS observation. For reference, XRD results (not cross-sectional views) of sintered bronze are shown in the figure. Bornite was also detected as shown in **Figure 11**. The figure shows the results of XRD for the sintered sulfide-dispersed bronze.

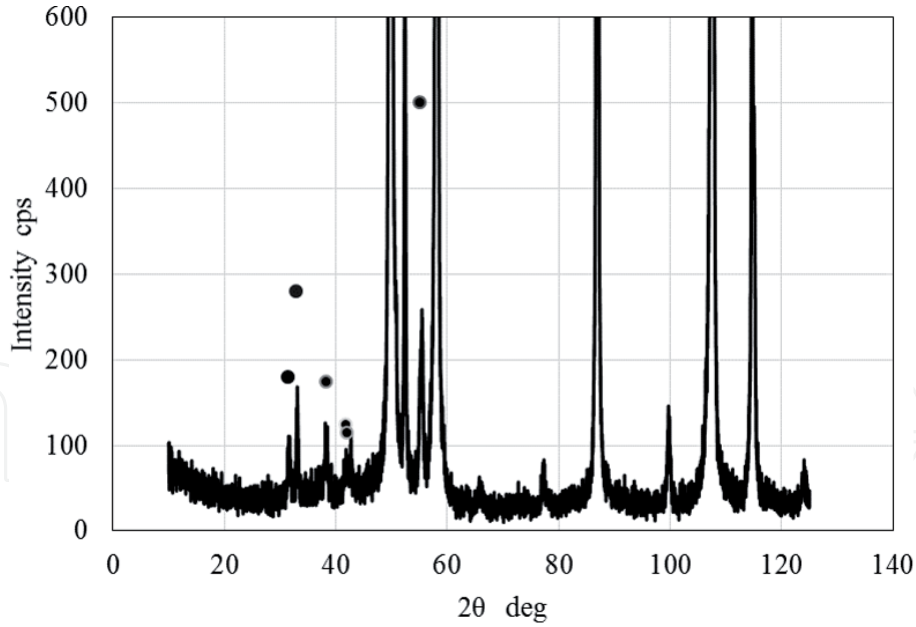

Figure 11.
XRD of sintered sulfide-dispersed bronze.

3.3.4 Hardness

Figures 12 and **13** show the Vickers hardness values of steel specimens and sintered copper alloys. As shown in **Figure 12**, the hardness of steel was almost the same during sintering and rolling. For steel, these thermal and operating conditions did not affect to change their microstructure and strength. It was important that the bimetallic bushing does not change the properties of the steel. As a result, manufacturing conditions were suitable for bimetal. As shown in **Figure 13a**–**c**, the results were divided into three categories depending on the sintering atmosphere. For all of the test groups that received their initial sintering, the high Sn content alloys are harder in each group. It is known that the Cu-Sn alloy becomes hard when the Sn content increases within the range of the Sn content of the test piece examined in this study. As a result, the basic characteristics of the Cu-Sn alloy in the sintered Cu alloy and the sulfide content in the Cu alloy had almost no influence on the hardness of the base material. After the rolling step, some samples became harder, but the other samples were not hard.

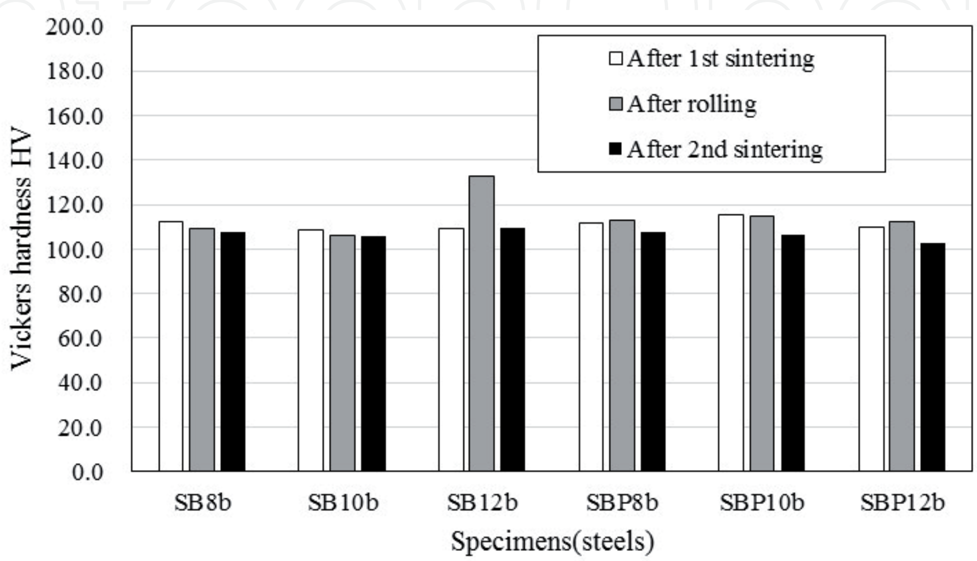

Figure 12.
Vickers hardness of steels under inert atmosphere [10].

The increase in hardness of some specimens may be the result of work hardening during rolling, and the lack of increase in hardness of other specimens may be a result of the destruction of the interface formed by solid diffusion between the powders.

When the hardness of SB group and SBP group after the second sintering is compared, Sn group is harder than Sn content (viz., 8, 10, 12 mass% Sn). After the second sintering, Cu_3Sn which was one of the intermetallic compounds was precipitated or crystallized. In this series, liquid sintering may occur during sintering. As a result, matrices with low tin content become softer after sintering.

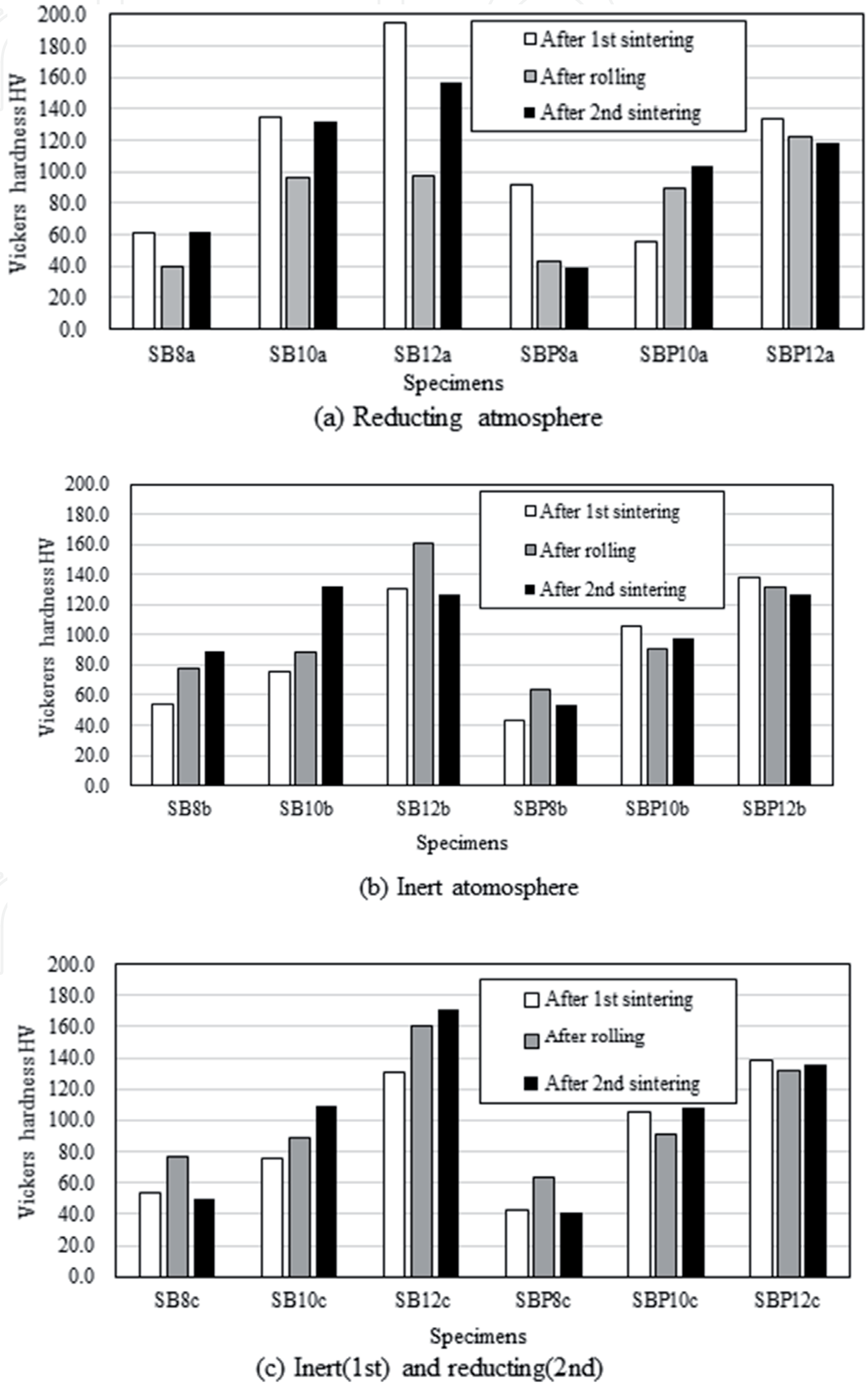

Figure 13.
Vickers hardness of Cu matrix [10].

Moreover, some specimens only sintering under inert atmosphere shown in **Figure 13b** were not harder than specimens only sintering under reduced atmosphere shown in **Figure 13a**, relatively. Reducing atmosphere might progress sintering under the same sintering temperature.

From these results, by using pre-alloyed atomizing bronze-containing sulfides, decreasing mechanical properties as hardness were not observed.

3.4 Summary

The effect of sulfur or sulfide on the mechanical properties of bronze specimens sintered under reducing inert gas atmosphere was investigated by subjecting water-atomized sulfide-dispersed bronze specimens to sintering. Furthermore, solid-phase sintering and liquid sintering were compared for the same Sn content. By using pre-alloyed atomizing bronze-containing sulfides, no mechanical properties were observed that decreased significantly as hardness. The sulfide content of the specimens decreased during sintering in a reducing atmosphere. With regard to mechanical properties such as hardness, the Sn content affected the properties regardless of whether the specimen had undergone solid-phase sintering or liquid sintering. In contrast, the sulfur and sulfide content and mechanical properties had no correlation.

4. Friction properties of sulfide bronze

In this study, tribological properties of copper alloys with sulfide particles are discussed. Friction characteristics were measured under dry and lubricated conditions to evaluate the effect of sulfide particles. Graphite penetrating into the pores caused improved tribological properties [11].

4.1 Materials and experimental procedure

4.1.1 Materials

The developed lead-free material is based on bronze-type Cu-Sn alloy and contains sulfide. For friction materials that use a sintering process, sulfides are considered to be an alternative element to lead, tested as TP-L (Cu-10 Sn-10 Pb mass%: lead bronze) and TP-A1 (Cu-12.15 Sn-1.78 Fe-0.48 S mass%) and for the purpose of comparing tribological properties using new materials prepared as TP-B1 (Cu-11.93 Sn-1.44 Fe-1.78 S mass%). The test specimen is sintered and rolled onto a steel plate, and the powder is separated. This plate was heated in furnace under reduction condition. In order to sinter to make the bimetal, the powder on the plate has to be heated at 1113 K for 10 min. After sintering, reduce the thickness of the plate by rolling, then sinter the rolled bimetallic, and roll again under the same conditions used in the initial.

4.1.2 Friction test

The friction test was performed using a ring on disk tester. The contact load was applied by its own weight and was in the range of 50–600 N. Disk specimens were attached to a shaft driven by a DC motor. The sliding speed could be controlled continuously in the range of 0.1–1.4 m/s. Mineral oil (approximately 30 μL, three drops from a microsyringe) is delivered to the interface just prior to testing. The disk surface was first contacted with the ring, and then the disk specimen was driven.

The laboratory air and the laboratory environment under the break-in process had a load of 20 N and were applied at a sliding distance of 120 m before testing. These specimens and carbon steel disks (S45C) were mirror finished. The roughness was Ra 0.025 μm (TP-L), Ra 0.167 μm (TP-A), Ra 0.343 μm (TP-B), and Ra 0.004 μm (carbon steel).

After interrupting at 20 N for 10 min in operating mode (friction distance 120 m), gradually load the ring in 50 N increments until a friction coefficient of 0.2 is reached or strange noise occurs. In the lubricant test, PAO (50 cSt @ 313 K) was used as a lubricant. Another test was performed on this material for high speed and low load [12].

4.2 Results and discussion

Friction coefficient during the test was shown in **Figure 14**. In the beginning of the test, lower friction coefficient of around 0.05 was measured in TP-B.

Friction coefficient of TP-L also shows a low coefficient of friction at the beginning of the test. After that, the friction coefficient abruptly increases at a load of 300 N. The friction coefficient between TP-A and TP-B is reduced at 200 and 300 N load. From the result, these sintered specimens could achieve a lower coefficient of friction.

Lubricating oil seems to hinder the formation of S-based coatings. Due to the pores passing through the lubricating oil, the difference in coefficient of friction is not so wide between the dry test and the lubricating oil test.

From **Figure 15a–d**, surface state after the test was observed. Attachment to the ring (carbon steel/S45C) of the copper alloy particles (TP-B) which is a part of the disk is observed (see the circle in **Figure 15b**). On the other hand, adhesion of the part of carbon steel to the disk was observed as shown in **Figure 15c**. The adhesion of the Cu alloy to carbon steel achieves a lower coefficient of friction than the adhesion of carbon steel to Cu alloy at high loads. These phenomena also reported another kind of friction test as sulfides play a role as solid lubricants [13].

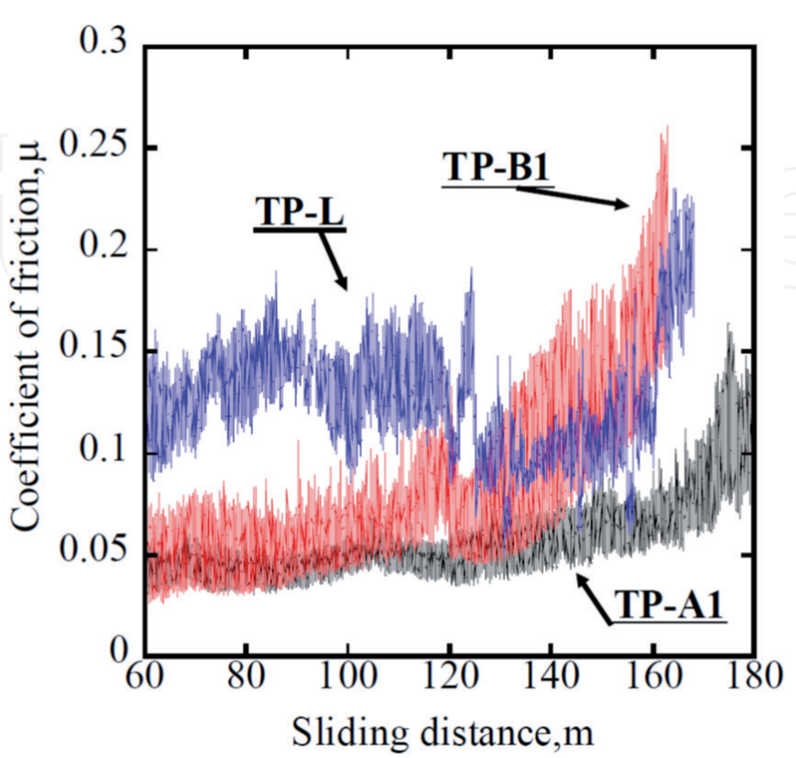

Figure 14.
Results of friction test [11].

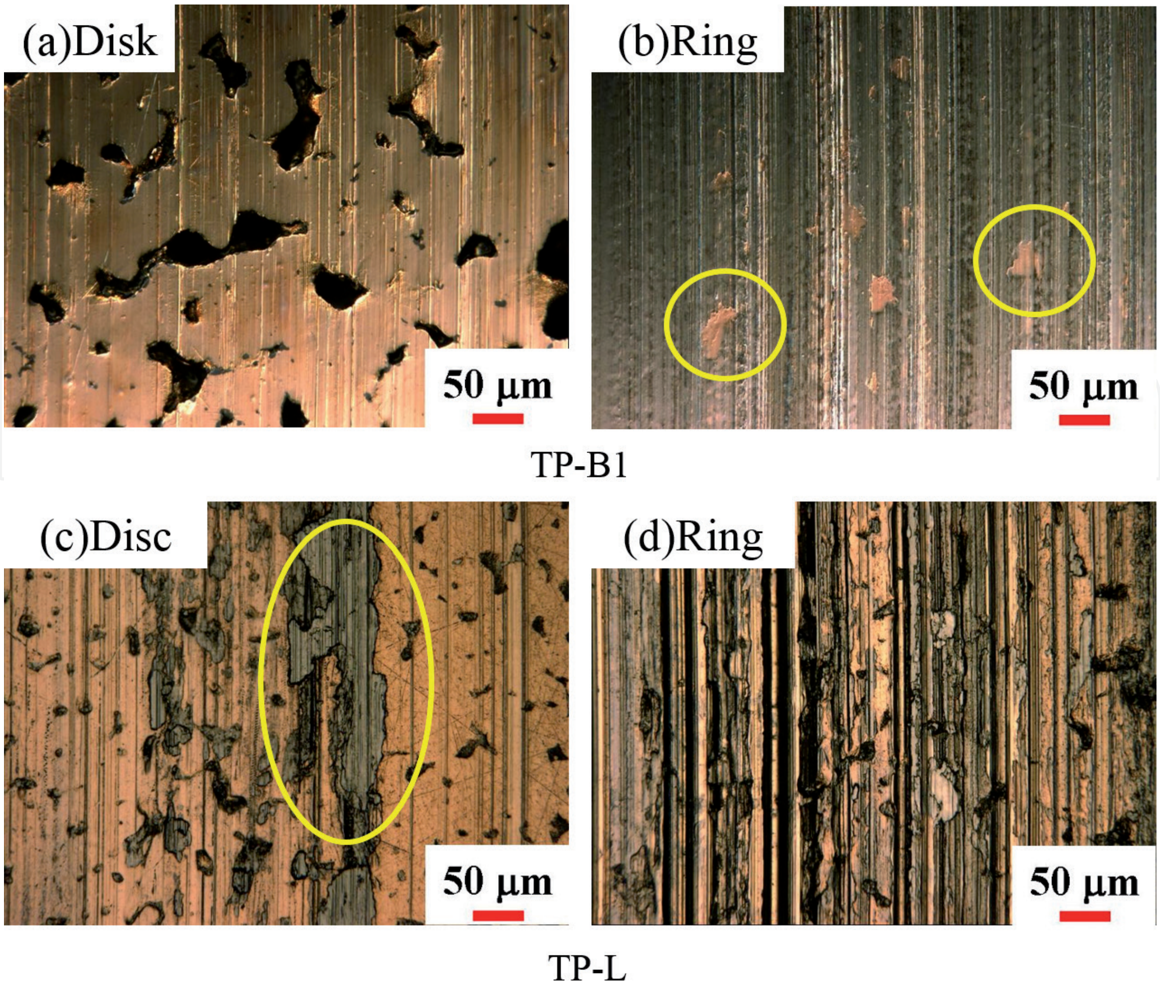

Figure 15.
Surface of disks and rings after the test [11].

In particular, MoS_2 was a common solid lubricant. Mixed MoS_2 in the Cu-based sintered material had better friction characteristics [14]. The sliding mechanism of MoS_2 is well known, and it is possible that a born person has the same or similar sliding mechanism as MoS_2 [15–17].

4.3 Summary

A friction test was conducted on the developed sintered Cu alloy-containing sulfide particles. The friction performance of the developed material was compared with those containing lead. The following is a summary of the results obtained.

The change in coefficient of friction depends on the behavior of the adhesive layer, especially under high load.

Sulfide-dispersed porous sintered Cu alloy realizes stabilization of friction coefficient at higher load than lead bronze.

5. Conclusions

In this study, we discussed how it affects already atomized bronze sulfide. Specifically, the strength of bronze matrix and the reaction between sulfide and hydrogen gas are drawing attention. We will clarify the composition and atmosphere effective for sintering bronze with sulfide dispersed. As a result, copper sulfide can sinter several types of atmosphere such as inert, reducing, and vacuum. In many reducing conditions, attention is paid to the disappearance of sulfides from the matrix. However, the sulfide itself did not affect the hardness of the matrix. Sulfide works as a solid lubricant instead of lead because it shows high seizure resistance during friction testing.

Conflict of interest

The authors declare that they have no conflicts of interest.

Author details

Tomohiro Sato
Kansai University, Suita-shi, Osaka, Japan

*Address all correspondence to: tom_sato@kansai-u.ac.jp

References

[1] Maruyama T, Abe H, Hirose K, Matsubayashi R, Kobayashi T. Influence of alloying elements on sulfide formation in lead free bronze castings with dispersed sulfide particles. Materials Transactions. 2012;**53**(2):380-384

[2] Taha MA, E-Mahallawy NA, Mousa TM, Hamouda RM, Yousef AFAG. Microstructure and castability of lead-free silicon brass alloys. Materialwissenschaft und Werkstofftechnik. 2012;**43**(8):699-704

[3] Dudek MA, Sidhu RS, Chawla N. Novel rare-earth-containing lead-free solders with enhanced ductility. The Journal of the Minerals, Metals & Materials Society. 2006;**58**:57-59

[4] Oksane VT, Lehtovaara AJ, Kallio MH. Load capacity of bismuth bronze bimetal bearing in lubricated conditions. Proc. of the 17th Nordic Symposium on Tribology. 2016;**222**:1-13

[5] Maruyama T, Wakai H, Kobayashi T. Some properties of sulfide dispersed lead free copper alloy castings, AFS transactions. Transactions of the American Foundry Society. 2008;**116**:299-307

[6] Lukas H, Fries SG, Sundman B. Computational Thermodynamics: The Calphad Method. New York, NY, USA: Cambridge University Press; 2007

[7] Sato T, Hirai Y, Kobayashi T. Development of lead free bronze with sulfide dispersion for sliding members. International Journal of Metal Casting. 2017;**11**(1):148-154

[8] Shikata H, Funabashi N, Ebine Y, Hayasaka T. Performance of sintered Cu-Sn-Ni bearings containing MoS_2. Modern Developments in Powder Metallurgy. 1985;**17**:497-512

[9] Sato T, Hirai Y, Maruyama T, Kobayasi T, Kurimoto, Ltd. Copper alloy for sliding materials. US Patent 8906129; 2014

[10] Sato T, Hirai Y. Effects of sulfur and tin contents on hardness of copper-tin alloy under reduced atmosphere in sintering process. Mechanical Engineering Journal. 2016;**3**(1):15-00704

[11] Sato T, Hirai Y, Fukui T, Tanizawa K, Usami H. Tribological properties of porous Cu based alloy containing nano sized sulfide particles. Journal of Advanced Mechanical Design Systems and Manufacturing. 2012;**6**(1):158-167

[12] Sato T, Hirai Y, Fukui T, Akiyama K, Usami U. Effects of dispersed sulfides in bronze under line contact conditions. Jurnal Tribologi. 2016;**8**:1-11

[13] Sato T, Hirai Y, Maruyama T, Kobayashi T. Sintering processes of Pb-Free copper alloy for friction materials. In: Proceedings of Powder Metallurgy World Congress and Exhibition 2010; 10-14 October 2010; Florence. Vol. 2. EPMA; 2010. pp. 313-319

[14] Kovalchenko AM, Fushchich OI, Danyluk S. The tribological properties and mechanism of wear of Cu-based sintered powder materials containing molybdenum disulfide and molybdenum diselenite under unlubricated sliding against copper. Wear. 2012;**290**:106

[15] Hirai Y, Sato T, Usami H. Combined effects of graphite and sulfide on the tribological properties of bronze under dry conditions. Journal Tribologi. 2016;**11**:14-23

[16] Hirai Y, Sato T, Usami H. Tribological properties of sintered

bronze containing micro-sized Sulfide. Journal of Japanese society of Tribologists. 2016;**61**:857-865

[17] Hirai Y, Ogawa K, Sato T, Usami H. Effect of machining history on tribological properties of bronze containing micro-sized Sulfide. Key Engineering Materials. 2017;**749**:246-250